This is a peer-reviewed, accepted author manuscript of the following conference paper: Tian, Qiuyang et al. "Data-driven control design for UAV autolanding: a pitch-only case study". 2024 3rd Conference on Fully Actuated System Theory and Applications (FASTA). Piscataway, NJ: IEEE. 2024, 1493-1497. https://doi.org/10.1109/FASTA61401.2024.10595378

Data-driven control design for UAV autolanding: a pitch-only case study

Qiuyang Tian[1], Weiwen Chen[1], Zelin Wang[1], Mingxuan Sun[3], Bo Zhu[1*], Laibing Jia[4], Tianjiang Hu[1,2*]

1. School of Aeronautics and Astronautics, Sun Yat-Sen University, Shenzhen 518107, China
E-mail: { tianqy3, chenww59, wangzlin25, zhubo5, hutj3} @mail2.sysu.edu.cn

2. School of Artificial Intelligence, Sun Yat-Sen University, Zhuhai 519000, China

3. College of Information Engineering, Zhejiang University of Technology, Hangzhou 310023, China
E-mail: mxsun@zjtu.edu.cn

4. Department of Naval Architecture, Ocean and Marine Engineering, University of Strathclyde, UK
Email: l.jia@strath.ac.uk

Abstract: This paper aims at exploring a new-type mode for autolanding control of fixed-wing unmanned aerial vehicles (UAVs). A discrete-time data-driven control scheme is tentatively proposed and developed with its pitch-only channel as a case study. Eventually, data-driven controllers inspired by attracting laws are introduced for a series of difference models. Numerical simulation for pitch-only dynamics is demonstrated to validate and compare performances of proposed DDC laws. Simulation results indicate that DDC laws can achieve the desired performance by altering data-driven models with different orders.

Key Words: Data-driven control, characteristic model, attracting laws (ALs)

1 Introduction

Fixed-wing unmanned aerial vehicles (UAVs) have numerous applications in fields including agriculture, traffic surveillance, industrial accident monitoring, crime prevention, assessment and restoration of nature reserve areas [1-5], etc. Compared with unmanned helicopters, multi-rotor aircraft, flapping-wing aircraft, and other aircraft, fixed-wing UAVs have advantages such as large payload, high speed, low energy consumption, long range, and high safety [6-7]. The increasing demand for tasks such as aerial reconnaissance, communication relays, resource exploration, and border surveillance, combined with the rapid advancements in technologies such as structural engineering, flight control algorithms, and power systems, are driving the development of fixed-wing UAVs toward greater autonomy and intelligence capabilities [8-9]. As the utilization of fixed-wing aircraft becomes more popular, there are more and more reported incidents of varying severities Autolanding is responsible for almost half of UAV accidents due to its vulnerability to destruction or damage during landing. This trend emphasizes developing more robust and adaptable control strategies to counteract modeling uncertainties and external disturbances that may arise during autolanding [10-11].

The autolanding trajectory traditionally consists of three phases: approach, glide, and flare [12-13]. An effective autolanding algorithm for fixed-wing UAVs should be capable of accurately and stably tracking the designated landing trajectory throughout all landing stages. Although linear model-based approaches are practical only within narrow ranges surrounding operation points, numerous studies have demonstrated the possibility of developing automatic landing algorithms for UAVs using decoupled longitudinal and lateral linear models [14-16]. The gain scheduling method is introduced to widen operational ranges by adjusting pre-designed control parameters for varying operation points to overcome this limitation. However, interpolated parameters generated by gain scheduling cannot always guarantee the stability of the closed-loop system [17]. Many nonlinear control techniques have also been studied in autolanding, but their effectiveness still depends significantly on the complexity and accuracy of dynamic models [18-19].

Data-driven control approaches, which do not rely on actual system dynamics, have gained interest due to the challenges faced by the above methods [21-26]. DDC methods aim to use only input/output (I/O) data to design control laws. In designing control laws for fixed-wing UAVs, uncertainties arising from model errors and environmental influences, such as wind disturbances and aerodynamic changes, cannot be neglected. DDC methods can adapt well to model uncertainties because they fully utilize historical data, including data from disturbed conditions. The concept of data-driven modeling originated from the characteristic modeling approach [24]. One significant difference is that the data-driven modeling method transforms nonlinear systems into linear systems with a single lumped, unmodeled term instead of various time-varying coefficients. Besides, DDC laws can be obtained from different data-driven models with similar structures, which means that few modifications are required to adapt controllers to new application scenarios, making the design process simpler and more convenient.

This paper discusses the application of DDC methods in UAV autolanding. Motivated by attracting laws, DDC laws are derived with guaranteed stability and error bounds from models of different orders. The main contributions of this study include: 1) the longitudinal motion of fixed-wing UAVs is introduced and analyzed, and the data-driven modeling on pitch-only dynamics is derived; 2) DDC laws are designed for data-driven models with different orders; 3) a numerical simulation is performed to demonstrate the application of DDC laws for tracking desired trajectories.

*This work is supported by National Natural Science Foundation of China under Grant 61973327 and the Royal Society's International Exchanges 2021 Cost Share NSFC.

2 Data-driven modeling for pitch-only dynamics of one fixed-wing UAV

This section presents data-driven modeling for the pitch-only dynamics. The mathematical model of a fixed-wing aircraft comprises several coupled non-linear equations that can be found in published literature. These coupled terms can be sufficiently small when the fixed-wing UAV is in steady-state flight. As a result, the dynamic model of a fixed-wing can be decomposed into longitudinal and lateral motions. Our study focuses on the longitudinal dynamics of a fixed-wing UAV, specifically its pitch-only model, which describes vertical rotation during the autolanding procedure. Disturbances and uncertainties arising from unmodeled dynamics due to decoupling can be rejected using appropriate control strategies.

The longitudinal autopilot for autolanding typically uses the throttle for airspeed and the elevator for pitch control. The inertial and body frames mentioned in this section are illustrated in Fig. 1, represented by O_I and O_B. When the airspeed reaches the desired value in a trimmed condition, the elevator δ_e is utilized to adjust the pitch angle θ and pitch rate q. Thus, the pitch-only equation for longitudinal motion is expressed as follows:

$$\begin{cases} \dot{\theta} = q \\ \dot{q} = \mathrm{M} \ / \ J_{yy} \end{cases} \tag{1}$$

where J_{yy} is the moment of inertia, and M is the pitch moment that is shown as follows:

$$\begin{aligned} \mathrm{M} \ &= \frac{1}{2}\rho_{air} V_a{}^2 Sc \\ &\times \left(C_{\mathrm{M}_0} + C_{\mathrm{M}_\alpha}\alpha + C_{\mathrm{M}_q}\frac{c}{2V_a}q + C_{\mathrm{M}_{\delta_e}}\delta_e \right) \end{aligned} \tag{2}$$

where C_{M_0}, C_{M_α}, and C_{M_q} are aerodynamic coefficients; α is the angle of attack; ρ_{air} is the air density; S is the planform area and c is the mean chord of the fixed-wing, respectively. By combining Eq.(1) and Eq.(2), the equation for pitch-only dynamics can be derived as follows:

$$\begin{aligned} \ddot{\theta} = &\frac{\rho_{air} V_a{}^2 Sc}{2J_{yy}} \left(C_{\mathrm{M}_q}\frac{c}{2V_a}\dot{\theta} + C_{\mathrm{M}_{\delta_e}}\delta_e \right) \\ &+ \frac{\rho_{air} V_a{}^2 Sc}{2J_{yy}} \left(C_{\mathrm{M}_0} + C_{\mathrm{M}_\alpha}\alpha \right) \end{aligned} \tag{3}$$

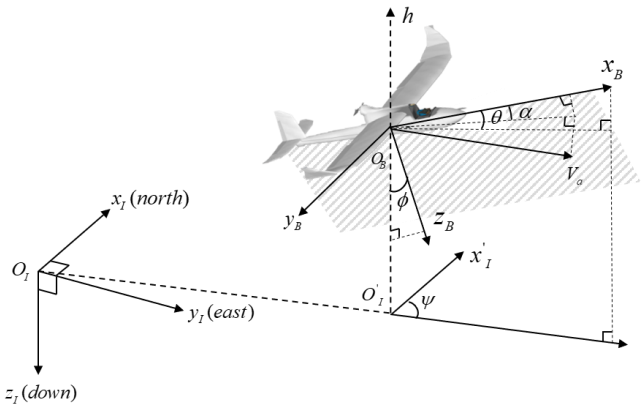

Fig. 1. Illustration of frames and state variables

To discretize the pitch-only dynamics, the following backward differences are utilized:

$$\begin{aligned} \dot{\theta} &\triangleq \theta(k) - \theta(k-1) / h \\ \ddot{\theta} &\triangleq \left(\theta(k+1) - 2\theta(k) + \theta(k-1) \right) / h^2 \end{aligned} \tag{4}$$

where k is the discrete time instance; h is the sampling period. The data-driven model for pitch-only dynamics can be expressed as

$$\begin{aligned}\theta(k+1) = {} & f_{\theta,1}\theta(k) + f_{\theta,2}\theta(k-1) \\ & + g_\theta \delta_e(k) + \varepsilon_\theta(k)\end{aligned} \tag{5}$$

where $f_{\theta,1}$, $f_{\theta,2}$ and g_θ are constant parameters; $\varepsilon_\theta(k)$ is the unmodeled term:

$$f_{\theta,1} = 2 + \frac{\rho_{air} V_a{}^2 S c^2 C_{\mathrm{M}_q}}{4 J_{yy} V_a} h$$

$$f_{\theta,2} = -1 - \frac{\rho_{air} V_a{}^2 S c^2 C_{\mathrm{M}_q}}{4 J_{yy} V_a} h$$

$$g_\theta = \frac{\rho_{air} V_a{}^2 S c C_{\mathrm{M}_{\delta_e}}}{2 J_{yy}} h^2$$

Consider first-order and second-order differences of the unmodeled term $\varepsilon_\theta(k)$:

$$\begin{aligned}\nabla\varepsilon_\theta(k) &= \varepsilon_\theta(k) - \varepsilon_\theta(k-1) \\ &= h\varepsilon_\theta^1(t_k) \\ \nabla^2\varepsilon_\theta(k) &= \nabla\varepsilon_\theta(k) - \nabla\varepsilon_\theta(k-1) \\ &= h^2\varepsilon_\theta^2(t_k)\end{aligned} \tag{6}$$

where $\varepsilon_\theta^1(t_k)$ and $\varepsilon_\theta^2(t_k)$ are derivatives lie within sampling points. Eq.(6) indicates that backward differences are bounded if respective derivatives are bounded. If the disturbance signal $\varepsilon_\theta(k)$ is a polynomial function of time, its derivatives can be seen as signals that change slowly over time. For example, it is seen that $\nabla\varepsilon_\theta = 0$, when ε_θ is a constant signal; $\nabla^2\varepsilon_\theta = 0$, as ε_θ is a ramp signal. Therefore, higher-order data-driven models are widely utilized to effectively reject disturbances caused by unmodeled terms because it is easier to estimate slow-changing signals than fast-changing ones. Typical higher-order data-driven models, such as first-order and second-order models, can be derived by transforming Eq.(5) into difference equations:

$$\begin{aligned}\nabla\theta(k+1) = {} & f_{\theta,1}\nabla\theta(k) + f_{\theta,2}\nabla\theta(k-1) \\ & + g_\theta\nabla\delta_e(k) + \nabla\varepsilon_\theta(k) \\ \nabla^2\theta(k+1) = {} & f_{\theta,1}\nabla^2\theta(k) + f_{\theta,2}\nabla^2\theta(k-1) \\ & + g_\theta\nabla^2\delta_e(k) + \nabla^2\varepsilon_\theta(k)\end{aligned} \tag{7}$$

3 Control design based on data-driven models

This section presents a design methodology for DDC based on data-driven models. The pitch-only controller's primary objective is to accurately follow the desired pitch angle produced by the outer-loop controller, like the altitude autopilot. The tracking error $e(k)$ is defined by

$$e(k) = \theta_d(k) - \theta(k) \tag{8}$$

where $\theta_d(k)$ represents the desired pitch signal. By applying the attracting law, the discrete-time dynamic of the tracking error defined by Eq.(8) can be designed as

$$e(k+1) = (1-\rho)e(k) \tag{9}$$

where $\rho \in (0,1)$ is a tunable parameter. According to Eq.(9), the relationship between $e(k+1)$ and $e(k)$ satisfies $|e(k+1)| < |e(k)|$, which indicates that the tracking error $e(k)$ decreases as time steps increase. Combining Eq.(5), Eq.(8) and Eq.(9), we have

$$\begin{aligned} e(k+1) &= \theta_d(k+1) - \theta(k+1) \\ &= \theta_d(k+1) - f_{\theta,1}\theta(k) + f_{\theta,2}\theta(k-1) \\ &\quad + g_\theta \delta_e(k) + \varepsilon_\theta(k) \\ &= (1-\rho)e(k) \end{aligned} \tag{10}$$

The ideal data-driven control law $\bar{\delta}_e(k)$ can be derived from Eq.(10):

$$\begin{aligned} \bar{\delta}_e(k) = \frac{1}{g_\theta}\big[&-(1-\rho)e(k) + \theta_d(k+1) \\ &- f_{\theta,1}\theta(k) - f_{\theta,2}\theta(k-1) - \varepsilon_\theta(k)\big] \end{aligned} \tag{11}$$

However, the ideal control law Eq.(11) is not realizable because the disturbance $\varepsilon_\theta(k)$ is unknown. A simple estimation $\hat{\varepsilon}_\theta(k)$ of the disturbance signal $\varepsilon_\theta(k)$ is its time-delay signal $\varepsilon_\theta(k-1)$ which yields:

$$\begin{aligned} \hat{\varepsilon}_\theta(k) = \theta(k) &- f_{\theta,1}\theta(k-1) \\ &- f_{\theta,2}\theta(k-2) - g_\theta \delta_e(k-1) \end{aligned} \tag{12}$$

Thus, the practical data-driven control law $\delta_e(k)$ is given as follows:

$$\begin{aligned} \delta_e(k) = \frac{1}{g_\theta}\big[&-(1-\rho)e(k) + \theta_d(k+1) \\ &- f_{\theta,1}\theta(k) - f_{\theta,2}\theta(k-1) - \hat{\varepsilon}_\theta(k)\big] \end{aligned} \tag{13}$$

According to Eq.(6), if the first-order difference $\nabla\varepsilon_\theta(k)$ is bounded, the maximum norm of $\nabla\varepsilon_\theta(k)$ can be noted by $\nabla\varepsilon_{\theta_{\max}}$. The closed-loop system Eq.(5) governed by DDC law is stable, and the upper limit of tracking error is bounded:

$$\overline{\lim_{k\to\infty}}|e(k)| \le \frac{\nabla\varepsilon_{\theta_{\max}}}{\rho} \tag{14}$$

For data-driven models Eq.(7) with higher-order differences, the 1-order DDC and 2-order DDC can be designed as:

$$\begin{aligned} \delta_e(k) = \delta_e(k-1) &+ \frac{1}{g_\theta} \\ &\times\big[-(1-\rho)e(k) + \theta_d(k+1) - \theta(k) \\ &- f_{\theta,1}\nabla\theta(k) - f_{\theta,2}\nabla\theta(k-1) - \nabla\hat{\varepsilon}_\theta(k)\big] \end{aligned} \tag{15}$$

and

$$\begin{aligned} \delta_e(k) = \delta_e(k-1) + \nabla\delta_e(k-1) &+ \frac{1}{g_\theta} \\ &\times\big[-(1-\rho)e(k) + \theta_d(k+1) - \theta(k) - \nabla\theta(k) \\ &- f_{\theta,1}\nabla^2\theta(k) - f_{\theta,2}\nabla^2\theta(k-1) - \nabla^2\hat{\varepsilon}_\theta(k)\big] \end{aligned} \tag{16}$$

where estimations for $\nabla\varepsilon_\theta(k)$ and $\nabla^2\varepsilon_\theta(k)$ are given by:

$$\begin{aligned}\nabla\hat{\varepsilon}_\theta(k) &= \nabla\theta(k) - f_{\theta,1}\nabla\theta(k-1)\\ &\quad - f_{\theta,2}\nabla\theta(k-2) - g_\theta\nabla\delta_e(k-1)\\ \nabla^2\hat{\varepsilon}_\theta(k) &= \nabla^2\theta(k) - f_{\theta,1}\nabla^2\theta(k-1)\\ &\quad - f_{\theta,2}\nabla^2\theta(k-2) - g_\theta\nabla^2\delta_e(k-1)\end{aligned} \tag{17}$$

4 Numerical Simulation

This section presents the results from numerical simulation to demonstrate the properties and effectiveness of the data-driven controllers. For the scenario of UAV autolanding, consider the pitch-only dynamics Eq.(3) with following parameters：

$$\begin{aligned}&m = 1\,\text{kg},\ g = 9.81\,\text{m/s}^2,\ \rho_{air} = 1.29\,\text{kg/m}^3\\ &S = 0.123\,\text{m}^2,\ c = 0.1\,\text{m},\ J = 0.0092\,\text{m}\times\text{kg}^2\\ &C_{\text{M}_0} = 0.0026,\ C_{\text{M}_q} = -0.0003,\ C_{\text{M}_{\delta_e}} = -0.0051\end{aligned}$$

The airspeed is set to 20 m/s , and the sampling time h is chosen as 0.001 s . As a consequence, constant parameters given by Eq.(5) can be computed as follows:

$$f_{\theta,1} = 1.999997,\ f_{\theta,2} = -0.999997,\ g_\theta = -0.008862$$

The desired pitch trajectory is set as a constant signal $\theta_d(k) = 0.15$ rad , while the disturbance $\varepsilon_\theta(k)$ is assumed to be a sine wave signal $\varepsilon_\theta(k) = 0.05*\sin(20\pi k\Delta t)$ rad . The initial states and control input for numerical simulation are assumed as follows:

$$\begin{aligned}&\theta(0) = 0.1\,\text{rad}, \nabla\theta(0) = \nabla^2\theta(0) = 0\,\text{rad},\\ &\delta_e(0) = \nabla\delta_e(0) = \nabla^2\delta_e(0) = 0\,\text{rad},\end{aligned}$$

To achieve a clear comparison, the 0-order,1-order, and 2-order DDC laws use the same tunable parameter ρ , which is set to 0.5.

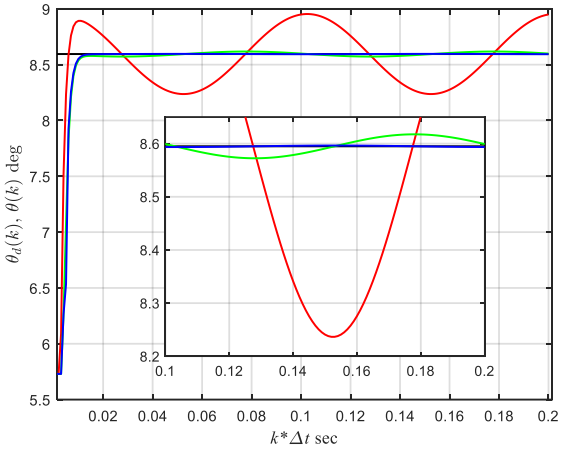

Fig. 2. Desired pitch angle $\theta_d(k)$ (black) and tracking trajectories $\theta(k)$ by using 0-order (red), 1-order (green) and 2-order (blue) DDC laws

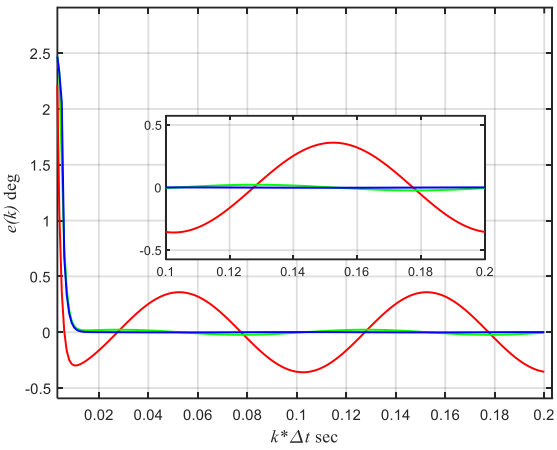

Fig. 3. Tracking errors $e(k)$ by using 0-order (red), 1-order (green) and 2-order (blue) DDC laws

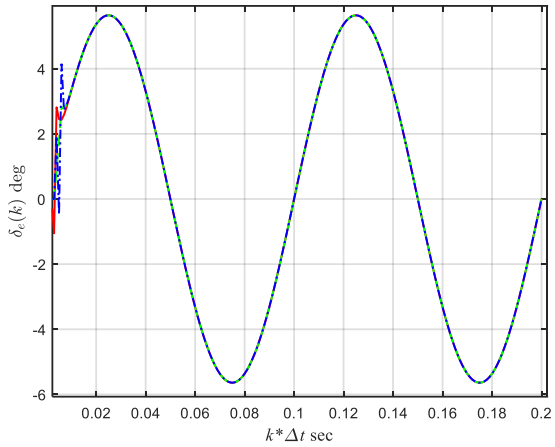

Fig. 4. Control inputs $\delta_e(k)$ of 0-order (red solid), 1-order (green dashed) and 2-order (blue dash-dot) DDC laws

According to numerical simulation results presented in Figs. 2-3, all tracking errors decrease rapidly within a short period of time. The 1-order DDC law yields better results than the 0-order DDC law while obtaining the similar performance as the 2-order DDC law. The tracking error of the 0-order DDC law is significantly influenced by the maximum absolute value of $\varepsilon_\theta(k)$ that can be approximated by $\nabla\varepsilon_{\theta_{\max}}/\rho$. Recorded data from numerical simulation indicates that absolute values of unmodeled terms with different differences satisfy $\varepsilon_{\theta_{\max}} \gg \nabla\varepsilon_{\theta_{\max}} > \nabla^2\varepsilon_{\theta_{\max}}$. It means that the upper limit of the tracking error gets smaller when a higher order data-driven model is chosen.

5 Conclusions

In this paper, a data-driven control (DDC) design method is tentatively proposed and developed for the autolanding of fixed-wing UAVs. The longitudinal pitch-only channel of UAV flights is concentrated on as a case study. Three DDC laws based on different difference models have been explored. Optimizing DDC laws can be achieved by selecting different models, while parameter tuning is simple with only one parameter. Numerical simulation shows that DDC laws can effectively govern pitch-only dynamics for closed-loop tracking with predictable error bounds. For practical implementation, it is suggested to use a lower order difference model that balances the performance of tracking error and system band. Further study is required to explore DDC schemes on UAV autolanding for lateral control loops and coupled systems.

References

[1] Yuan, Huali, et al. Design and testing of a crop growth sensor aboard a fixed-wing unmanned aerial vehicle[J]. *Computers and Electronics in Agriculture.* 2022. 194: 106762.

[2] Wang, Liang, Fangliang Chen, and Huiming Yin. Detecting and tracking vehicles in traffic by unmanned aerial vehicles[J]. *Automation in construction*. 2016, 72: 294-308.

[3] Hu, Shuyan, et al. Disguised tailing and video surveillance with solar-powered fixed-wing unmanned aerial vehicle[J]. *IEEE Transactions on Vehicular Technology*. 2022 71(5): 5507-5518.

[4] El Tin, Fares, Inna Sharf, and Meyer Nahon. Fire Monitoring with a Fixed-wing Unmanned Aerial Vehicle[J]. *IEEE 2022 International Conference on Unmanned Aircraft Systems* (ICUAS). pp. 1350-1358.

[5] Yuan, Xin, et al. Deep Reinforcement Learning-Driven Reconfigurable Intelligent Surface-Assisted Radio Surveillance with A Fixed-Wing UAV[J]. *IEEE Transactions on Information Forensics and Security*. 2023, 18: 4546-4560.

[6] Trittler, Martin, Thomas Rothermel, and Walter Fichter. Autopilot for landing small fixed-wing unmanned aerial vehicles with optical sensors[J]. *Journal of Guidance, Control, and Dynamics*. 2016,39(9): 2011-2021.

[7] Lungu, Mihai. Backstepping and dynamic inversion combined controller for auto-landing of fixed wing UAVs[J]. *Aerospace Science and Technology*. 2020, 96: 105526.

[8] Thurrowgood, Saul, et al. A biologically inspired, vision- based guidance system for automatic landing of a fixed- wing aircraft[J]. *Journal of Field Robotics*. 2014, 31(4): 699-727.

[9] Ambati, Pradeep R., and Radhakant Padhi. Robust auto-landing of fixed-wing UAVs using neuro-adaptive design[J]. *Control Engineering Practice*. 2017, (6): 218-232.

[10] Zhao, Shulong, et al. A novel data-driven control for fixed-wing UAV path following[C]. *IEEE 2015 International Conference on Information and Automation*. pp. 3051-3056.

[11] Liang, Shaojun, et al. Data-driven fault diagnosis of FW-UAVs with consideration of multiple operation conditions[J]. *ISA transactions*, 2022, 126: 472-485.

[12] Wu, H., Hu, J. Theory, Methods and Applications of Characteristic Modeling, in Chinese[M]. *National Defense Industry Press*, Beijing, 2019.

[13] Warren, Michael, et al. An Automated Emergency Landing System for Fixed- Wing Aircraft: Planning and Control[J]. *Journal of Field Robotics*. 2015, 32(8): 1114-1140.

[14] Ahsan, Mansoor, et al. Performance comparison of two altitude-control algorithms for a fixed-wing UAV[C]. *2013 3rd IEEE International Conference on Computer, Control and Communication (IC4)*. IEEE, 2013.

[15] Anjali, B. S., A. Vivek, and J. L. Nandagopal. Simulation and analysis of integral LQR controller for inner control loop design of a fixed wing micro aerial vehicle (MAV)[J]. *Procedia Technology* 25 (2016): 76-83.

[16] Sedlmair, Nicolas, Julian Theis, and Frank Thielecke. Flight testing automatic landing control for unmanned aircraft including curved approaches[J]. *Journal of Guidance, Control, and Dynamics* 45.4 (2022): 726-739.

[17] Rugh, Wilson J., and Jeff S. Shamma. Research on gain scheduling[J]. *Automatica.* 36.10 (2000): 1401-1425.

[18] Zhang, Qingrui, and Hugh HT Liu. Robust nonlinear close formation control of multiple fixed-wing aircraft[J]. *Journal of Guidance, Control, and Dynamics* 44.3 (2021): 572-586.

[19] Li, Yu, et al. A cascaded nonlinear fault-tolerant control for fixed-wing aircraft with wing asymmetric damage[J]. *ISA transactions* 136 (2023): 503-524.

[20] Reinhardt, Dirk, and Tor Arne Johansen. Control of fixed-wing uav attitude and speed based on embedded nonlinear model predictive control[J]. *IFAC-PapersOnLine* 54.6 (2021): 91-98.

[21] Baldi, S., Sun, D., Xia, X., Zhou, G., & Liu, D. (2022). ArduPilot-based adaptive autopilot: architecture and software-in-the-loop experiments[J]. *IEEE Transactions on Aerospace and Electronic Systems*, 58(5), 4473-4485

[22] Hashjin, Saeid Aghaei, et al. Data-driven model-free adaptive current control of a wound rotor synchronous machine drive system[J]. *IEEE Transactions on Transportation Electrification* 6.3 (2020): 1146-1156.

[23] Gao, Han, et al. Forecasting-based data-driven model-free adaptive sliding mode attitude control of combined spacecraft[J]. *Aerospace Science and Technology* 86 (2019): 364-374.

[24] Wu, H., Hu, J., & Xie, Y. Characteristic model-based all-coefficient adaptive control method and its applications[J]. *IEEE Transactions on Systems, Man, and Cybernetics, Part C (Applications and Reviews)*. 2007, 37(2), 213-221. Doi: 10.1109/TSMCC.2006.887004

[25] Sun, M., Wu, L., Hu, Y., & Zhou, W. (2017). Digital control strategies with attractiveness and invariance specifications[J]. *IEEE Transactions on Control Systems Technology*, 26(4), 1272-1284.

[26] Sun, M., Li, W., & Wu, L. (2021). Dead-beat terminal sliding-mode control: A guaranteed attractiveness approach[J]. *Automatica*, 129, 109609.